

Electrodeposition of indium onto Mo/Cu for the deposition of Cu(In,Ga)Se₂ thin films

R.C. Valderrama^a, M. Miranda-Hernández^{a,1}, P.J. Sebastian^{a,*}, A.L. Ocampo^b

^a Centro de Investigación en Energía, Universidad Nacional Autónoma de México, Temixco 62580, Morelos, Mexico

^b Facultad de Química, Universidad Nacional Autónoma de México, Ciudad Universitaria 04510, Mexico, D.F., Mexico

Received 30 July 2007; received in revised form 17 November 2007; accepted 19 November 2007

Available online 4 December 2007

Abstract

A study of the electrodeposition and the oxidation process of indium on Mo/Cu substrates from a bath containing 0.008 M InCl₃, 0.7 M LiCl at pH 3 is described in this work. The voltamperometric study showed a reduction process which corresponds to the conversion of In³⁺ to In⁰ and an oxidation process which takes place in different steps. Utilizing the chronoamperometric technique the total efficiency of process, the number of monolayers, the film thickness and the diffusion coefficient were evaluated. The analysis of current transients, using theoretical growth model, showed that the electrodeposition of indium adjusts to a three-dimensional growth under instantaneous nucleation limited by diffusion. The kinetic growth parameters were evaluated through a non-linear fit. The films were characterized by X-ray diffraction and scanning electron microscopy techniques. These studies showed that the films were of crystalline in nature with compact and uniform surface, even for the film with a deposition time of 1 min.

© 2007 Elsevier Ltd. All rights reserved.

Keywords: Indium; Electrodeposition; Nucleation and growth; CuIn alloy; Cu(In,Ga)Se₂

1. Introduction

Despite a number of publications that refer to the electrodeposition (ED) of CuInSe₂ (CIS) thin films, only a few reports have been published on a systematic study of the growth and incorporation of the elements during the ED of the films. Mishra and Rajeshwar [1] were the first to publish the CIS film formation mechanism, concluding that CIS films grow on an initial deposit of Cu_{2-x}Se. Another important contribution was made by Thouin et al. [2,3], who suggested that the stoichiometry of the CIS film is controlled by the ratio between selenium and copper fluxes ([Se⁴⁺]/[Cu²⁺]) on the electrode which in turn controls the insertion of In by the Kroger's mechanism between excess Se in the copper selenide (Cu_xSe_y) film and In ions. The CIS film is precursor to the quaternary phase Cu(In,Ga)Se₂ (CIGS) and for a long time the formation of CIGS by ED in one step was

not well understood, as it was very difficult to incorporate the Ga into the standard range of potential in which the CIS electrodeposition was commonly carried out. Bhattacharya et al. [4] were the first to demonstrate the Ga incorporation by ED, but at very low levels. To get the device quality films it was necessary to supplement the films by physical vapor deposition of Cu, In, and Ga up to 50% of the total film thickness. Calixto et al. [5] reported that bath concentration affects the composition of electrodeposited CIGS films. A bath ratio of [Se⁴⁺]/[Cu²⁺] equals to 1.75 was required for maintaining the suitable deposit levels of Se and Cu, while [In³⁺] could be adjusted to control the deposits of In and Ga.

With the purpose of knowing more about the film formation mechanism of Cu(In,Ga)Se₂ obtained through the ED technique, a systematic study on the growth and incorporation of the elements using the electrocrystallization theories reported in the literature [6–10] is suggested. It is proposed to study the nucleation and growth process of: In, Ga, Cu–Se, In–Ga–Se and Cu–In–Ga–Se. In this paper, the electrodeposition of In is presented. The study was carried out not only because of our interest in In as a component in CIGS films, but also because of its relevant role as In oxide [11–15] due to its application

* Corresponding author at: Centro de Investigación en Energía, Universidad Nacional Autónoma de México, Xochicalco s/n, Temixco 62580, Morelos, Mexico. Tel.: +52 55 56229841; fax: +52 55 56229742.

E-mail address: sjp@cie.unam.mx (P.J. Sebastian).

¹ ISE member.

in optoelectronic devices. Another motivation for this study is that it has rarely been studied as a pure metal [16–18]. This work provides a systematic study of the electrodeposition of In utilizing electrochemical method, its characterization by X-ray diffraction and scanning electron microscopy (SEM) techniques.

2. Experimental details

The experimental system for the deposition of the indium films constituted an electrochemical cell of three electrodes connected to a PGZ301 potentiostat, for application of the potential difference. The data acquisition was carried out by means of the Voltmaster 4 software. For CIGS growth on Mo it is important to make a good ohmic contact between the semiconductor and the substrate. However, $[\text{In}^{3+}]$ does not present good adhesion on Mo, and for that reason it was necessary to deposit a layer of Cu on Mo substrate (Mo/Cu) in order to deposit In. The electrodeposition of Cu layer on Mo was carried out using a bath containing 1 M CuCl_2 , 0.7 M LiCl, pH 1.7 and an applied potential of -0.30 V/SCE for 1 min. In order to ensure reproducible interface conditions, a fresh sample of Mo/Cu was used for each study. The counter electrode used was a platinum mesh of area larger than the working electrode, and the reference electrode was a saturated calomel electrode (SCE, $E_0 = -0.24$ V). The electrolyte consisted of 0.008 M InCl_3 and 0.7 M LiCl at pH 3, prepared with de-ionized water (Ultrapure Milli-Q). The electrolyte was de-oxygenated for 30 min with pure N_2 , before initiating the measurements and was maintained during the experiment.

The cyclic voltammetry technique was used to describe the potential intervals where the reduction and oxidation processes of In^{3+} appear. For these tests a scan of different potential values starting from the negative limiting potential ($E_{-\lambda}$) was done. That is, from the rest potential ($E_0 = 0.0$ V vs. SCE) increases by each 20 mV in the negative direction until reaching the $E_{-\lambda} = -1.0$ V versus SCE at a scan rate of 8 mV/s, whereas the positive limiting potential stayed constant at 0.05 V versus SCE.

The chronoamperometric technique was used to evaluate the different stages of electrodeposition of In on Mo/Cu substrate, by applying a double pulse potential for 20 s, which varies the electrocrystallization potential. The potentials were selected considering the results of the voltammetric study.

The structure of the films was studied by means of X-ray diffractometer (Rigaku, DMAX 2200) using Cu $K\alpha$ radiation (1.54056 \AA). The morphology of the films was analyzed by SEM (Leo 1450VP) at 20 kV. The XRD and SEM characterization of the films were done within 24 h of their deposition.

3. Results and discussion

3.1. Voltamperometric study

In order to select the interval of potential in which the reduction of In^{3+} would be carried out, the cyclic voltammetry technique was used, by varying the negative limiting potential ($E_{-\lambda}$). The purpose of varying this potential in small increments was to systematically describe the evolution of the electrodeposition process.

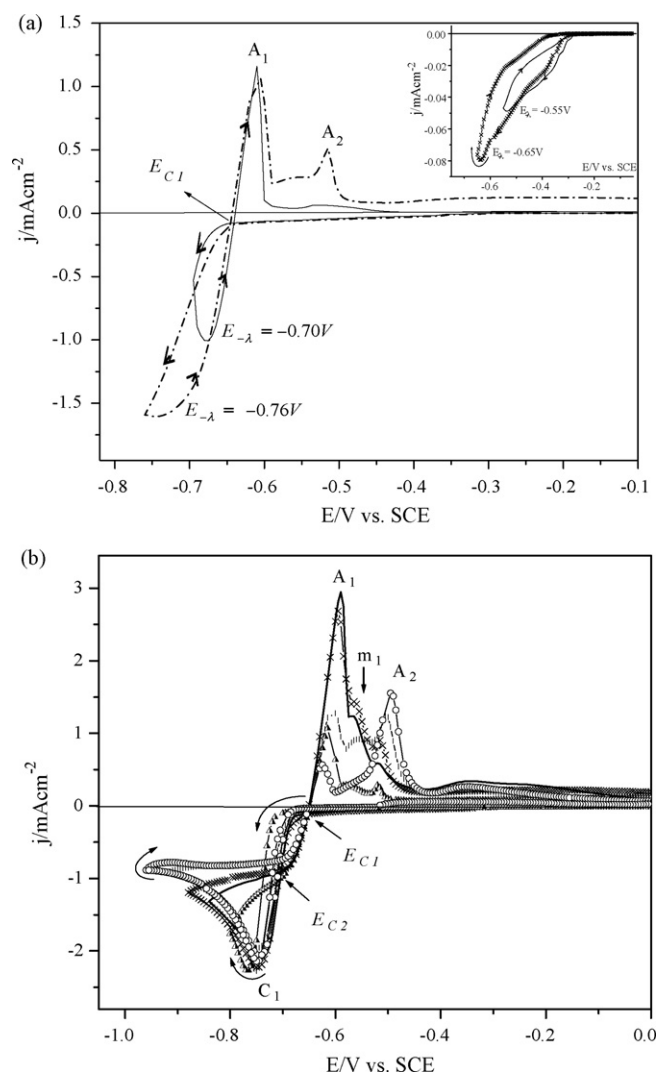


Fig. 1. Typical voltammograms obtained during In deposition on Mo/Cu electrodes in 0.008 M InCl_3 , 0.7 M LiCl (pH 3) bath, at a scan rate of 8 mV/s, for different negative limiting potentials, $E_{-\lambda}$. (a) (—) -0.70 V and (---) -0.76 V, inset: (—) -0.55 V and (---) -0.65 V; (b) (Δ) -0.80 V, (—) -0.84 V, (\times) -0.88 V, (\square) -0.92 V and (\circ) -0.96 V.

Fig. 1 shows the typical voltammogram of Mo/Cu electrode in 0.008 M InCl_3 , 0.7 M LiCl and pH 3 during the interval of -0.1 to -0.76 V (Fig. 1a) and for 0.0 to -0.96 V (Fig. 1b) at a scan rate of 8 mV/s. In the inset of Fig. 1a, for $E_{-\lambda} \geq -0.65$ V an important response of negative current density ($-j$) associated with a capacitive behavior was observed. During the reverse potential scan, the current density was of low magnitude, but different from zero, so that at these potentials the In deposition on Mo/Cu still does not take place. The In metallic deposition begins at $-0.76 \text{ V} < E_{-\lambda} \leq -0.70$ V versus SCE (Fig. 1a) with the manifestation of an important cathodic current density and a crossing potential (E_{C1}) at -0.65 V [19,20]. Also, an oxidation peak (A_1) at -0.61 V was observed which is attributed to the dissolution of recently formed In.

Fig. 1b shows a reduction peak (C_1) with one current density value practically independent of the applied potential, $E_{-\lambda}$ (see Table 1), the return scan presents a second crossing potential

Table 1
The potential and current density values corresponding to the reduction peak, C₁, and the oxidation peaks: A₁, A₂, and the parameter m₁, for the different imposed negative potentials, E_{-λ}, during In deposition on Mo/Cu

E _{-λ} (V vs. SCE)	Cathodic responses		Anodic responses					
	C ₁		A ₁		m ₁		A ₂	
	E (V vs. SCE)	-j (mA cm ⁻²)	E (V vs. SCE)	j (mA cm ⁻²)	E (V vs. SCE)	j (mA cm ⁻²)	E (V vs. SCE)	j (mA cm ⁻²)
-0.70	-0.67	-1.0	-0.61	1.8	-	-	-	-
-0.72	-0.69	-1.3	-0.61	0.6	-	-	-	-
-0.74	-0.69	-1.4	-0.61	0.9	-	-	-0.52	0.2
-0.76	-0.74	-1.6	-0.61	1.0	-	-	-0.51	0.5
-0.78	-0.73	-2.3	-0.60	1.4	-	-	-0.51	0.8
-0.80	-0.76	-2.2	-0.61	1.0	-	-	-0.52	0.2
-0.82	-0.74	-2.1	-0.61	1.5	-	-	-0.52	0.5
-0.84	-0.74	-2.1	-0.59	2.9	-0.56	1.2	-0.52	0.5
-0.86	-0.76	-2.0	-0.59	2.3	-0.56	1.2	-0.51	0.8
-0.88	-0.75	-2.2	-0.59	2.6	-0.56	1.4	-0.51	0.8
-0.90	-0.74	-2.0	-0.60	1.3	-0.56	1.0	-0.51	0.7
-0.92	-0.75	-2.0	-0.60	1.3	-0.56	0.9	-0.50	1.2
-0.94	-0.75	-2.2	-0.61	0.8	-	-	-0.50	1.2
-0.96	-0.74	-2.1	-0.62	0.5	-	-	-0.50	1.5
-0.98	-0.75	-2.1	-0.62	0.2	-	-	-0.49	2.0
-1.00	-0.76	-2.2	-0.62	0.2	-	-	-0.52	0.7

(E_{C2}) at ~-0.70 V, hence it may be inferred that the formation of In metallic nucleus is limited by a diffusion process of the electroactive species [19,20]. While, in the anodic region between A₁ and A₂ oxidation peaks, which were previously described, a current plateau (m₁) was defined.

With the purpose of to be able to describe the different steps which presented during the reduction/oxidation processes, Table 1 presents the values of potential and the current density that correspond to the cathodic and anodic responses for the imposed values of E_{-λ}. The electrodeposition of In on Mo/Cu begins from -0.70 and goes up to -1.0 V, so that, at -0.70 V it was under mixed control [21,22] and at -0.80 V < E_{-λ} ≤ -0.70 V it was controlled by diffusion process, at -1.0 V < E_{-λ} ≤ -0.80 V it was limited by diffusion, confirming the results described in the previous voltammograms. On the other hand, the oxidation process was carried out in different steps, which depends on the potential at which the metallic In was deposited. The oxidation process A₁ was presented at every potential interval studied; the value of the current density for A₁ showed an important behavior: it was increased for E_{-λ} in the potential interval -0.70 to -0.84 V and was decreased for E_{-λ} from -0.86 to -1.0 V, hence it may be inferred that A₁ corresponds to the dissolution of the In⁰ according to the reaction:



The potential for reaction (1) in agreement with the Nernst equation is

$$E' = E^0 + \frac{0.06}{3} \log |\text{In}^{3+}| \quad (2)$$

where |In³⁺| = 0.008 M and E₀ = -0.61 V versus SCE at pH 3 [23], therefore E' = -0.65 V versus SCE. If one compares the E⁰ value with the crossing potential E_{C1} = -0.65 V versus SCE

it can be observed that the potentials are very similar and their values agree with the magnitude of the conditional potential of the system where it is taken into account the experimental conditions, as expected for the redox pair of a system [9,10].

Whereas, A₂ oxidation peak appears when In⁰ has been formed at -0.74 V and considering the spontaneous formation of CuIn alloy at room temperature [24,25], therefore A₂ is associated to In dissolution from the CuIn alloy which was formed during the interval of potential shown in Table 1.

The results shown in Fig. 1 indicate that the In electrodeposition/dissolution mechanism, in the present work was carried out in two steps depending on the potential E_{-λ}, so that, when the energy conditions are higher than that for the instantaneous deposition of In⁰ part of this was diffused to the bulk Cu to form the CuIn alloy, fact by which the occurrence of two current maxima may be justified. Therefore, increase of positive current density for A₂ peak at more negative potentials than -0.74 V was recorded [26].

The potential interval of -0.70 to -0.85 V versus SCE from the previous voltamperometric study was selected to analyze the nucleation processes of In³⁺ in greater detail using the chronoamperometric technique.

3.2. Chronoamperometric study

In order to find out the different stages of the electrocrystallization process of In³⁺ on Mo/Cu substrates, double potential pulses were applied, so that, during the direct pulse the In deposition was carried out, which was dissolved during the reverse pulse.

Fig. 2 shows a family of potentiostatic current transients of the electrodeposition and oxidation for the In on Mo/Cu substrates in 0.05 M InCl₃, 0.7 M LiCl (pH 3) bath. The imposed direct pulses varied from -0.7 to -0.85 V, while the reverse pulse was

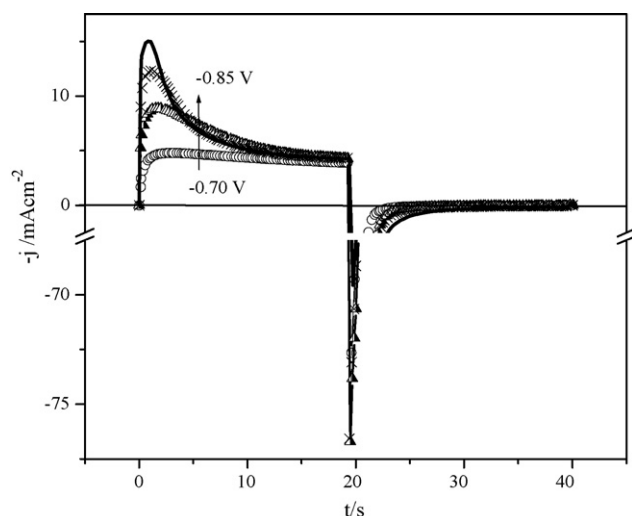


Fig. 2. The potentiostatic current transients for the deposition and oxidation of In on Mo/Cu substrates in 0.05 M InCl_3 and 0.7 M LiCl (pH 3) bath. The imposed direct pulses were (○) -0.70 V, (▲) -0.75 V, (×) -0.80 V and (—) -0.85 V vs. SCE, the inverse pulse stayed constant at $+0.10$ V vs. SCE.

maintained constant at $+0.10$ V, the pulse time was 20 s. During the In deposition (first 20 s) the shape of the transients is a typical response of an electrochemical nucleation and growth process. A sudden increase of current until reaching a maximum value, then it decreases asymptotically until reaching a constant current value.

Considering the current transients (Fig. 2), the efficiency of the process, the number of monolayers, the film thickness and the diffusion coefficient were evaluated. In order to evaluate the efficiency of the process, the charges associated with the reduction and oxidation processes, Q_C and Q_A , respectively, were obtained by integrating the cathodic and the anodic branches of the current transients. Table 2 shows the values for Q_A , Q_C and the total efficiency of the process (Q_A/Q_C ratio) for the different imposed potentials. These values, $Q_A/Q_C \cong 1$, indicate a high degree of reversibility for the In electrodeposition and oxidation.

An approximate way to evaluate the monolayers that were formed during the In deposition was formulated as follows: considering the number of In atoms required to cover the geometric area of the working electrode (1 cm^2) and if the area of an In atom is $\approx 8.66 \times 10^{-16} \text{ cm}^2$, therefore 1.15×10^{15} atoms of In will form a monolayer, thus the quantity of charge to form the monolayer would be $Q_{\text{monolayer}} = 0.185 \text{ mC}$. Finally, $Q_C/Q_{\text{monolayer}}$ ratio is equal to the number of monolayers (Table 2).

Table 2

The dependence of the reduction Q_C and oxidation Q_A charge, efficiency of process, Q_A/Q_C , the number of monolayers, and the film thickness, h , on the potential obtained from the current transient analysis presented in Fig. 2

E (V vs. SCE)	Q_C (mC cm^{-2})	Q_A (mC cm^{-2})	Q_A/Q_C	No. of monolayers	h (μm)
-0.70	82.9	85.3	1.03	448	4.50
-0.75	116.8	121.7	1.04	631	6.33
-0.80	124.2	129.4	1.04	671	6.74
-0.85	127.6	122.1	0.96	690	6.92

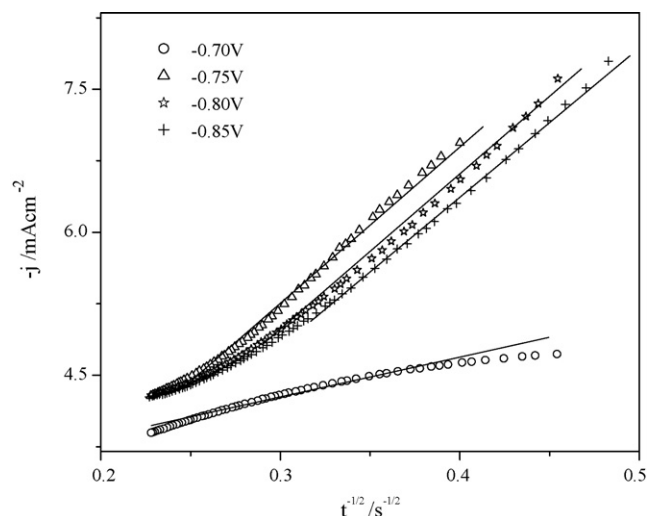


Fig. 3. The falling part of the transients from Fig. 2 plotted, $-j$ vs. $t^{-1/2}$, according to the Cottrell's equation predicting the linearity for diffusionally controlled. The symbols are experimental values and the lines represent the linear adjustments.

The film thickness was calculated according a Faraday's law normalized to a unit surface [14]:

$$F = \frac{MQ}{\rho zh} \quad (3)$$

where the number of electrons exchanged $z=3$ (Eq. (1)), charge $Q=Q_C$, h is the thickness, indium molar mass $M=114.82 \text{ g mol}^{-1}$ and density $\rho=7.31 \text{ g cm}^{-3}$. Substituting these values in Eq. (3) one gets h as a function of Q_C , which is

$$h = \frac{MQ}{\rho z F} = (5.426 \times 10^{-5}) Q_C \quad (4)$$

Table 2 indicates that both the number of monolayers and the value of h slowly increase with the imposed potential, with the exception of the values that correspond to $E=-0.70$ V.

The diffusion coefficient (D) was evaluated by analyzing the experimental data that corresponds to the fall of the direct pulse transients. This was plotted as $-j$ versus $t^{-1/2}$ (Fig. 3) and was observed that at longer times, the $-j$ values tend to come together in one point, and all responses can be fitted through a straight line with almost the same inclination, except for the case in which $E=-0.70$ V. This concurs with the linearity predicted by the Cottrell's equation. Thus, the linear fit was done according to the Cottrell's equation:

$$j = \frac{zFD^{1/2}c}{\pi^{1/2}} = mt^{-1/2} + b \quad (5)$$

Table 3
The dependence of current, J_m , and time, t_m , maxima, the diffusion coefficient, D , and the number density of nucleation active sites, N_0 , on the potential obtained from the current transients analysis presented in Fig. 2

E (V vs. SCE)	J_m (mA cm ⁻²)	t_m (s)	D ($\times 10^{-6}$ cm ² s ⁻¹)		N_0 (Eq. (7)) ($\times 10^5$ cm ⁻²)
			Cotrell's equation	Eq. (7)	
-0.70	4.80	3.04	0.21	1.90	5.86
-0.75	8.89	1.55	3.82	4.67	2.99
-0.80	12.35	1.08	4.01	4.39	6.69
-0.85	15.04	0.85	3.93	4.19	11.22

where z and F were defined in Eq. (3), c is the bulk concentration of species ($c = 5 \times 10^{-5}$ mol cm⁻³). Therefore D is give by,

$$D = \left[\frac{m(\pi t)^{-1/2} + b\pi^{-1/2}}{14.473 C \text{ cm}^{-3}} \right]^2 \quad (6)$$

In Table 3, the D values are shown as a function of potential. The average experimental value was $D = 3.9 \times 10^{-6}$ cm² s⁻¹.

In order to be able to study and describe the electrocrystallization process of In, the potentiostatic transients of Fig. 2 was analyzed. It has been reported in the literature similar responses to these transients, which have been evaluated through mathematical models that correspond to a three-dimensional growth [6,7]. In accordance with voltamperometric study and the evaluation of D ; the In deposit was controlled by a diffusion process. Thus, the transients in Fig. 2 can be described through a three dimensional growth (3D) for an instantaneous nucleation:

$$J = \frac{zFD^{1/2}}{\pi^{1/2}t^{1/2}} [1 - \exp(-N_0\pi KDt)] \quad (7)$$

Or for the progressive type nucleation:

$$J = \frac{zFD^{1/2}c}{\pi^{1/2}t^{1/2}} \left[1 - \exp\left(-\frac{2AN_0\pi KDt^2}{3}\right) \right] \quad (8)$$

N_0 is the number density of nucleation active sites (cm⁻²). A is the steady-state nucleation rate per active site (s⁻¹). The other terms are defined in Cotrell's equation, except K which is the non-dimensional growth rate constant of a nucleus, defined as

$$K = \left(\frac{8\pi Mc}{\rho} \right)^{1/2} \quad (9)$$

To determine whether the nucleation is instantaneous or progressive, an initial observational diagnostic was done, that involves comparing the experimental and theoretical transients in non-dimensional coordinates. For that, the experimental and theoretical transients are normalized by their corresponding maximum values of current (J_m) and time (t_m). In Table 3, the experimental values of J_m and t_m are given. Theoretical maximum values can be evaluated by equating the first derivative of Eqs. (7) and (8) to zero, then finding the values of t_m and J_m . So for the instantaneous case:

$$t_m = \frac{1.2564}{N_0\pi KD} \quad (10)$$

and

$$J_m = 0.6382zFDc(KN_0)^{1/2} \quad (11)$$

For the progressive case:

$$t_m = \left(\frac{4.6733}{AN_0\pi KD} \right)^{1/2} \quad (12)$$

and

$$J_m = 0.4615zFD^{3/4}c(KAN_0)^{1/4} \quad (13)$$

The non-dimension expression of Eqs. (7) and (8) for the instantaneous case is

$$\left(\frac{J}{J_m} \right)^2 = \frac{1.9542}{t/t_m} \left\{ 1 - \exp \left[-1.2564 \left(\frac{t}{t_m} \right) \right] \right\}^2 \quad (14)$$

And for the progressive case is

$$\left(\frac{J}{J_m} \right)^2 = \frac{1.2254}{t/t_m} \left\{ 1 - \exp \left[-2.3367 \left(\frac{t}{t_m} \right)^2 \right] \right\}^2 \quad (15)$$

Fig. 4 shows the normalized cathodic transients from Fig. 2 (symbols) together with the theoretical curves (lines) for instantaneous and progressive 3D nucleation and growth, obtained

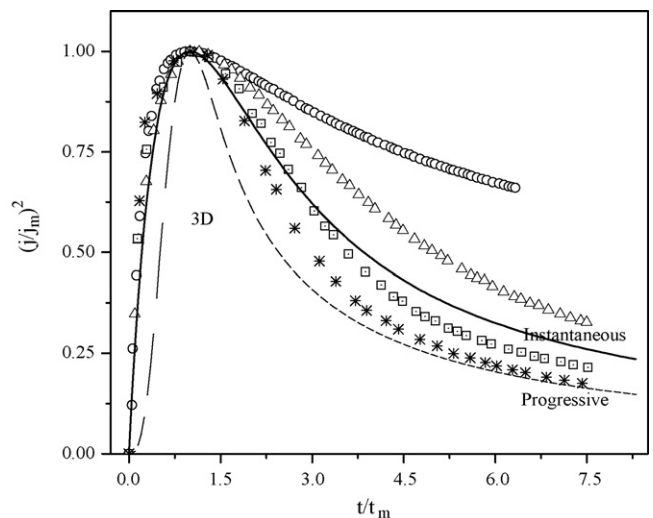


Fig. 4. A comparison of the theoretical non-dimensional plots, $(j/j_m)^2$ vs. (t/t_m) for instantaneous equation (14) (solid line) and progressive equation (15) (dashed line) nucleation with experimental data of the potentiostatic transients from Fig. 2. The imposed potentials were: (○) -0.70 V, (△) -0.75 V, (□) -0.80 V and (✱) -0.85 V.

using Eqs. (14) and (15), respectively. By comparing the experimentally obtained data with the theoretical curves, the figure shows that at a very short time, before reaching the maximum points, all of the experimental data follow the tendency of instantaneous nucleation. After for longer periods, during the current fall, the experimental curves were separated and when the imposed potential is more negative, the transient fall between the limits of instantaneous and progressive nucleation. Thus, it appears that the In deposition was carried out under a 3D growth with instantaneous nucleation.

In order to prove that the experimental transients correspond to a 3D growth with instantaneous nucleation, a non-linear fit of Eq. (7) was performed. Table 3 gives values for: D and N_0 , simulated from the fit of Eq. (7). In this table, values for the experimental D obtained through the Cottrell's equation, are also reported. By comparing the experimental D with the simulated one, similar values were found with the exception of $E = -0.70$ V. On the other hand, the kinetic parameter of nucleation N_0 increases while the applied potential pulse was more negative. This behavior was expected, since the density of active sites was favored when increasing the energetic conditions (potential), without considering the value of $E = -0.70$ V.

Finally, to show that the parameters reported in Table 3 correctly describe the experimental results, the simulated values for D and N_0 were substituted in Eq. (7), together with the known constants, including $K = 0.14$ (Eq. (9)). In this way the theoretical current transient was generated for each of the applied potentials (Fig. 5).

Fig. 5 shows a comparison between the simulated transients with the experimental ones obtained for the bath 0.05 M InCl_3 and 0.7 M LiCl (pH 3). When $E = -0.70$ V, the experimental values were adjusted to the model for $t < 4$ s, but for $t > 4$ s it is more adequate to use the D value obtained by the Cottrell's equations. The remaining experimental transients were adjusted very well with the simulated transients. Thus, the In deposition on Mo/Cu substrates in 0.05 M InCl_3 , 0.5 M LiCl and pH 3 was

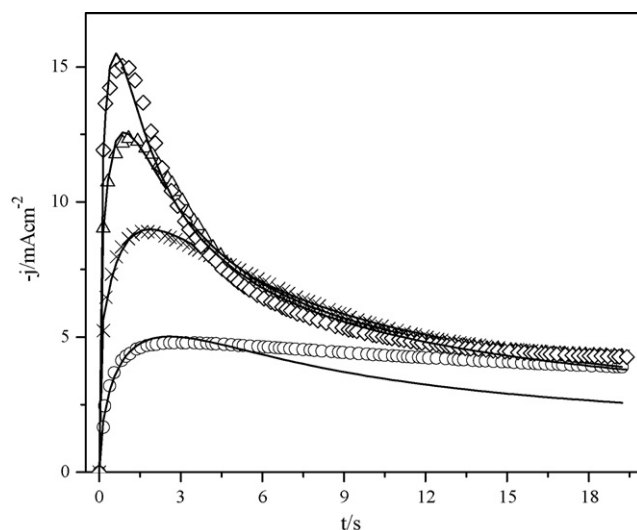


Fig. 5. A comparison of the simulated transients for the 3D instantaneous nucleation equation (7) (solid lines) with the experimental transients of the deposition of In on Mo/Cu substrates in 0.05 M InCl_3 , 0.7 M LiCl at pH 3. The imposed potentials were: (○) -0.70 V, (×) -0.75 V, (△) -0.80 V and (◇) -0.85 V vs. SCE.

carried out under a 3D growth with instantaneous nucleation limited by diffusion, which concurs with the reports by other authors [16,17] for the In system.

In all of the analyses carried out in the chronoamperometric study, it was found that the experimental transient that corresponds to -0.70 V differs from the values and the behavior reported for the other current transients. According to what was found in the voltamperometric analysis, the response at -0.70 V is presented under mixed control, therefore, the D value is very small compared to the rest and the adjustment was not reached.

To complement this study, In films, deposited at the same potentials and in the same electrochemical bath in which the chronoamperometric study was carried out, were analyzed using

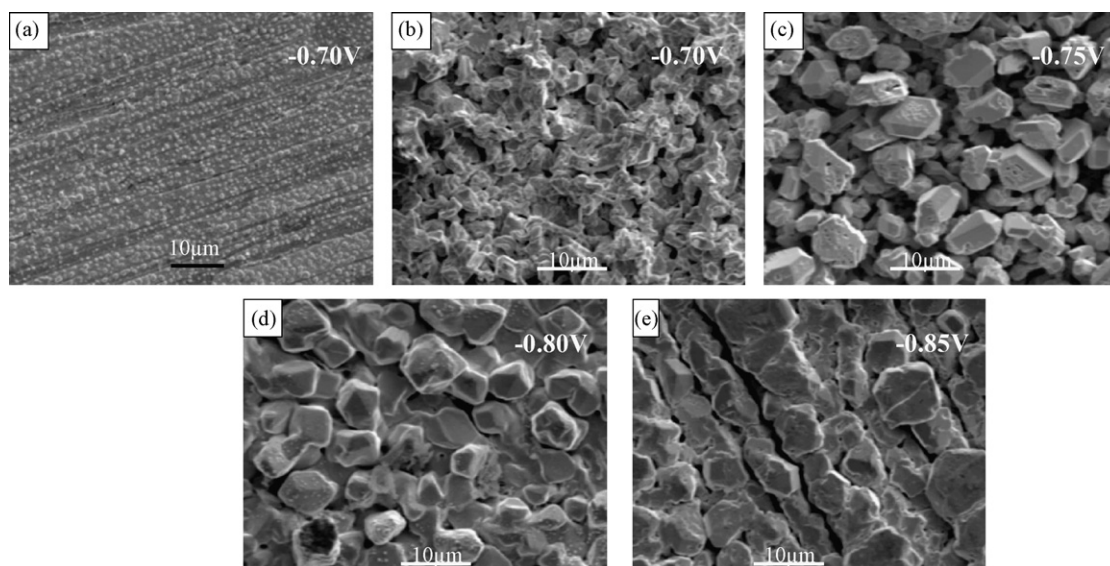


Fig. 6. The SEM images of In films deposited at different potentials on Mo/Cu substrates in 0.05 M InCl_3 , 0.7 M LiCl and pH 3. (a) At -0.70 V vs. SCE for 1 min. The images of (b)–(e) were deposited from -0.70 to -0.85 V vs. SCE for 30 min.

physical characterization techniques, in order to know the morphology and structure of the In films in terms of applied potential.

3.3. Physical characterization

To study the structure and morphology of the materials deposited, X-ray diffraction and scanning electronic microscopy were employed.

Fig. 6 shows five SEM images of In films obtained applying a pulse for different cathodic potentials, between -0.70 and -0.85 V versus SCE, at two different time intervals (1 and 30 min) on Mo/Cu substrates immersed in 0.05 M InCl_3 , 0.7 M LiCl and at pH 3. Fig. 6a corresponds to the film deposited at -0.70 V for 1 min. In Fig. 6a, a uniform deposit consisting of crystals of approximately $0.5 \mu\text{m}$ was observed. The samples show traces of the polishing lines, since the substrates were polished during the cleaning. Fig. 6b corresponds to the deposit at -0.70 V for 30 min. In this figure, a massive deposit was observed, which does not present a defined crystalline geometry. However, for the deposit at -0.75 V for 30 min (Fig. 6c), well-defined crystalline structures, separated with grain sizes that vary between 2 and $10 \mu\text{m}$ were observed. With the increase of the deposition potential (Fig. 6d and e), the crystals come together forming agglomerates that make up a compact surface. Also, when comparing the SEM image for the film deposited for 1 min (Fig. 6a) with those of 30 min, it is evident that the deposition time is a function of In grain size growth.

The results of the SEM analysis concur with those obtained from the study of current transients, since: 3D growths with instantaneous nucleation produce massive deposits, and also concurs with the calculation obtained for the thickness of these films ($h = 6 \mu\text{m}$).

Fig. 7 presents the XRD spectra for the In films deposited at different pulses of cathodic potentials between -0.70 and -0.85 V versus SCE for two deposition time intervals (1 and 30 min) on Mo/Cu substrates immersed in 0.05 M InCl_3 , 0.7 M LiCl and pH 3. The XRD analysis was done at an incident angle of 1.5° . In Fig. 7a, the films deposited at different potentials for 1 min are indicated within the figure. The XRD spectrum in Fig. 7a exhibits as first phase the CuIn alloy at 34.459° and 43.097° , according to the JCPDS card 35-1150. The peak that corresponds to the In phase at 32.985° is barely observable. Also, two peaks at 43.372° and 50.494° that correspond to the Cu substrate were observed.

Fig. 7b shows the XRD spectra for the films deposited at different potentials. This figure indicates that the films are polycrystalline in nature for all the deposition potentials. The first phase was In, without considering the known phase of Cu, in the (101) plane. This diffraction spectrum corresponds to the tetragonal system according to the JCPDS card 05-0642. The CuIn phase was presented as the second phase of importance.

Considering the results of XRD and SEM, the films deposited for 1 min presented a compact crystalline layer with In nucleuses which reacts with Cu forming CuIn alloy, on this the In film was deposited.

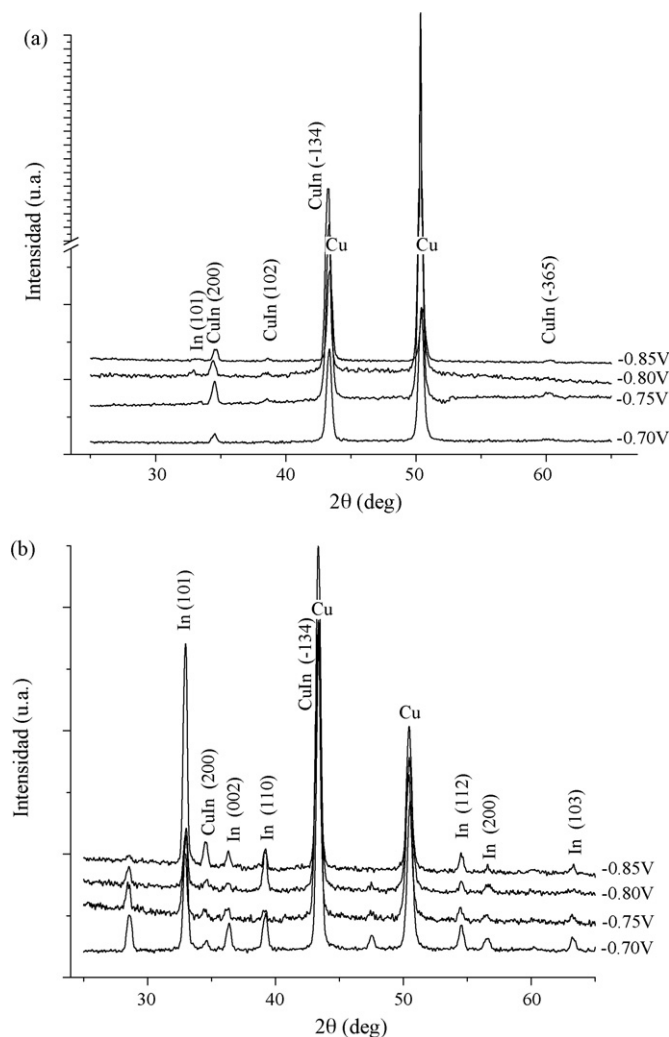


Fig. 7. The XRD patterns of In films deposited on Mo/Cu substrates in 0.05 M InCl_3 , 0.7 M LiCl and pH 3 at different potentials from -0.70 to -0.85 V vs. SCE for two different times: (a) 1 min and (b) 30 min. Angle of incidence is 1.5° .

4. Conclusions

The voltamperometric study showed a reduction process (peak C_1) which corresponds to the reaction of In^{3+} to In^0 . The oxidation peak A_2 corresponds to In dissolution from the CuIn alloy. Also, it can be noted that the experimental cross potential of In^{3+} to In^0 ($E_{C1} = -0.65$ V vs. SCE) was very close to the value reported in the literature ($E^0 = -0.61$ V vs. SCE). The nucleation of In was limited by the diffusion process.

The current transients were utilized to evaluate the charge associated with the oxidation and reduction process. From this it was observed that the efficiency of the process In^{3+} to In^0 was 100%. Also the physical parameters like number of monolayers (670 monolayers), the thickness of the film, and the diffusion coefficient ($D = 3.8 \times 10^{-6} \text{ cm}^2 \text{ s}^{-1}$) were evaluated. The analysis of the reduction part of the current transients, using theoretical growth model, showed that the electrodeposition of indium adheres to a 3D growth under instantaneous nucleation limited by diffusion. The kinetic growth parameters N_0 was eval-

uated through a non-linear fit. In addition to that the diffusion coefficient was also evaluated.

From the structural and morphological characterization it may be concluded that the films are of polycrystalline in nature with compact and uniform surface. In the first minute of deposition a compact layer of CuIn alloy was formed on that the In film was grown. After a 30 min deposition, large crystallites of In was formed and as the potential was increased agglomerates were formed, resulting in compact and massive surfaces.

The current transients showed 3D growth with instantaneous nucleation producing massive deposits. This is in good agreement with the results obtained from the physical characterization. A detailed study of the electrodeposition of In was carried out and the results obtained from this will help in analyzing the electrochemical behavior of In during the deposition of CIS and CIGS.

Acknowledgements

The authors gratefully acknowledge Ing. Francisco Ginez-Carbajal for helping with the electrodeposition of In films. This work was funded by DGAPA-UNAM under the grant ES113107.

References

- [1] K.K. Mishra, K. Rajeshwar, *J. Electroanal. Chem.* 271 (1989) 279.
- [2] L. Thouin, S. Massaccesi, S. Sanchez, J. Vedel, *J. Electroanal. Chem.* 374 (1994) 81.
- [3] L. Thouin, J. Vedel, *J. Electrochem. Soc.* 142 (1995) 2996.
- [4] R.N. Bhattacharya, H. Wiesner, T.A. Berens, R.J. Matson, J. Keane, K. Ramanathan, A. Swartzlander, A. Mason, R.N. Noufi, *J. Electrochem. Soc.* 144 (1997) 1376.
- [5] M.E. Calixto, K.D. Dobson, B.E. McCandless, R.W. Birkmire, *J. Electrochem. Soc.* 153 (2006) G521.
- [6] B. Scharifker, G. Hills, *Electrochim. Acta* 28 (1983) 879.
- [7] B. Scharifker, J. Mostany, *J. Electroanal. Chem.* 177 (1984) 146.
- [8] C. Nila, I. González, *J. Electroanal. Chem.* 401 (1996) 171.
- [9] M. Miranda-Hernández, I. González, *Electrochim. Acta* 42 (1997) 2295.
- [10] M. Miranda-Hernández, M. Palomar-Pardavé, N. Batina, I. González, *J. Electroanal. Chem.* 443 (1998) 81.
- [11] J.R. Bellingham, W.A. Phillips, C.J. Adkins, *Thin Solid Films* 195 (1991) 23.
- [12] D.-X. Dai, F.R. Zhu, I. Davoli, S. Stizza, *Appl. Surf. Sci.* 59 (1992) 195.
- [13] B.L. Kuzin, D.I. Bronin, A.Y. Neiman, A.G. Kozyntseva, G.K. Vdovin, S.V. Vakarin, V.G. Zyryanov, *Russ. J. Electrochem.* 33 (1997) 564.
- [14] S. Omanovic, M. Metikos-Hukovic, *Thin Solid Films* 458 (2004) 52.
- [15] A. El Sayed, S.S. Abd El Rehim, H. Manssur, *Monatsh. Chem.* 122 (1991) 1019.
- [16] G. Gunawardena, D. Pletcher, A. Razaq, *J. Electroanal. Chem.* 164 (1984) 363.
- [17] S.B. Saidman, E.C. Belloq, J.B. Bessone, *Electrochim. Acta* 35 (1990) 329.
- [18] R. Piercy, N.A. Hampson, *Electroanal. Chem. Interf. Electrochem.* 59 (1975) 261.
- [19] R.C. Barradas, F.C. Benson, S. Fletcher, *J. Electroanal. Chem.* 80 (1977) 305.
- [20] S. Fletcher, C.S. Halliday, D. Gates, M. Westcott, T. Levin, G. Nelson, *J. Electroanal. Chem.* 159 (1983) 267.
- [21] A. Radisic, A.C. West, P.C. Searson, *J. Electrochem.* 149 (2) (2002) C94.
- [22] Y. Cao, A.C. West, *J. Electrochem.* 149 (4) (2002) C223.
- [23] M. Pourbaix, *Atlas of Electrochemical Equilibria in Aqueous Solutions*, Pergamon Press, Oxford, 1974, p. 436.
- [24] J.R. Tuttle, A.M. Gabor, D.S. Albin, A. Tennant, M. Contreras, R. Noufi, *Proceedings of the Seventh Sunshine Project on Thin Film Solar Cells*, Tokyo, Japan, 1993.
- [25] S. Yamanaka, B.E. McCandless, R.W. Birkmire, *Proceedings of the 23rd IEEE PVSC*, Louisville, KY, USA, 1993.
- [26] M. Seo, M. Aihara, A.W. Hasselb, *J. Electrochem.* 148 (10) (2001) B400.